Significance of the occulter diffraction for the PROBA3/ASPIICS formation flight metrology

Landini, Federico, Bemporad, Alessandro, Focardi, Mauro, Fineschi, Silvano, Romoli, Marco, et al.

Federico Landini, Alessandro Bemporad, Mauro Focardi, Silvano Fineschi, Marco Romoli, Maurizio Pancrazzi, Cristian Baccani, Gerardo Capobianco, Davide Loreggia, Gianalfredo Nicolini, Giuseppe Massone, Vladimiro Noce, Cédric Thizy, Jean-Sébastien Servaye, Etienne Renotte, "Significance of the occulter diffraction for the PROBA3/ASPIICS formation flight metrology," Proc. SPIE 9604, Solar Physics and Space Weather Instrumentation VI, 96040E (21 September 2015); doi: 10.1117/12.2187916

SPIE.

Event: SPIE Optical Engineering + Applications, 2015, San Diego, California, United States

Significance of the occulter diffraction for the PROBA3/ASPIICS formation flight metrology

Federico Landini[a], Alessandro Bemporad[b], Mauro Focardi[a], Silvano Fineschi[b], Marco Romoli[c], Maurizio Pancrazzi[a], Cristian Baccani[c], Gerardo Capobianco[b], Davide Loreggia[b], Gianalfredo Nicolini[b], Giuseppe Massone[b], Vladimiro Noce[a], Cédric Thizy[d], Jean-Sébastien Servaye[d], Etienne Renotte[d]

[a]INAF - Osservatorio Astrofisico di Arcetri, Largo E. Fermi 5, Firenze, Italy;
[b]INAF - Osservatorio Astrofisico di Torino, Strada Osservatorio 20, Pino Torinese (Torino), Italy;
[c]Università di Firenze - Dipartimento di Fisica e Astronomia, Via Sansone 1, Sesto Fiorentino (Firenze), Italy;
[d]Centre Spatial de Liège, Université de Liège, Liege Science Park, 4013 Angleur, Belgium

ABSTRACT

PROBA-3/ASPIICS is a formation flying coronagraph selected by ESA and currently in its C/D phase. It is constituted by two spacecrafts (OSC, Occulter SpaceCraft, carrying the occulter, diameter 142 cm, and CSC, Coronagraph SpaceCraft, with the telescope) separated by ∼144 m, kept in strict alignment by means of an active custom system. The alignment active system most critical components are the Shadow Positioning Sensors (SPS), a series of Si-PM (Silicon Photomultiplier) measuring the penumbra generated by the occulter. The arrangement of the SPSs around the telescope entrance aperture is defined as a trade-off between mechanical constraints and maximum sensitivity to misalignments. The signal detected by the SPSs can be approximately simulated with a geometrical analysis based on the variation of the penumbra generated by the external occulter. The stray light generated by the diffraction from the external occulter may affect the SPSs signal. It is mandatory to carefully evaluate its level in order to refine the active alignment adjustment algorithm. This work is dedicated to the description of the preliminary investigation performed in order to evaluate the impact of the diffraction on the SPSs signal.

Keywords: Formation flying, Diffraction, Coronagraph, ASPIICS, SPS, Silicon Photomultipliers, Stray light, Solar Corona

1. INTRODUCTION

Since the first solar coronagraph, designed and built by Bernard Lyot in 1932,[1] it has been clear to the solar community that stray light is the main limitation to the observation of the inner corona. In fact, a solar coronagraph simulates a solar eclipse by occulting the solar disk with an opaque diaphragm, aiming at revealing a source of light that is more than 6 orders of magnitude fainter than the disk itself. The solar disk light diffracted by the diaphragm disturbs the observation, usually preventing the observation of the solar corona close to the disk limb.

As a matter of fact, no coronagraph has ever been able to get close to the solar eclipse observational conditions. PROBA-3/ASPIICS[2,3] is the first space-borne coronagraph that can achieve results comparable to those seen during solar eclipses. It consists of two formation flying (FF) spacecrafts, the coronagraph spacecraft (CSC) and the occulter spacecraft (OSC), separated by an average distance of 144.348 m. The external occulter EO, installed on the OSC, has a diameter of 1.42 m.

The telescope, carried by the CSC, is designed according to the classical Lyot[1] and Evans[4] principles and has an entrance pupil of 5 cm diameter. The solid angle subtended by the entrance pupil with respect to the diffracting

Further author information: (Send correspondence to F. Landini)
F. Landini: E-mail: flandini@arcetri.astro.it, Telephone: +39 (0)55 275 5221

Solar Physics and Space Weather Instrumentation VI, edited by Silvano Fineschi, Judy Fennelly, Proc. of SPIE Vol. 9604, 96040E · © 2015 SPIE
CCC code: 0277-786X/15/$18 · doi: 10.1117/12.2187916

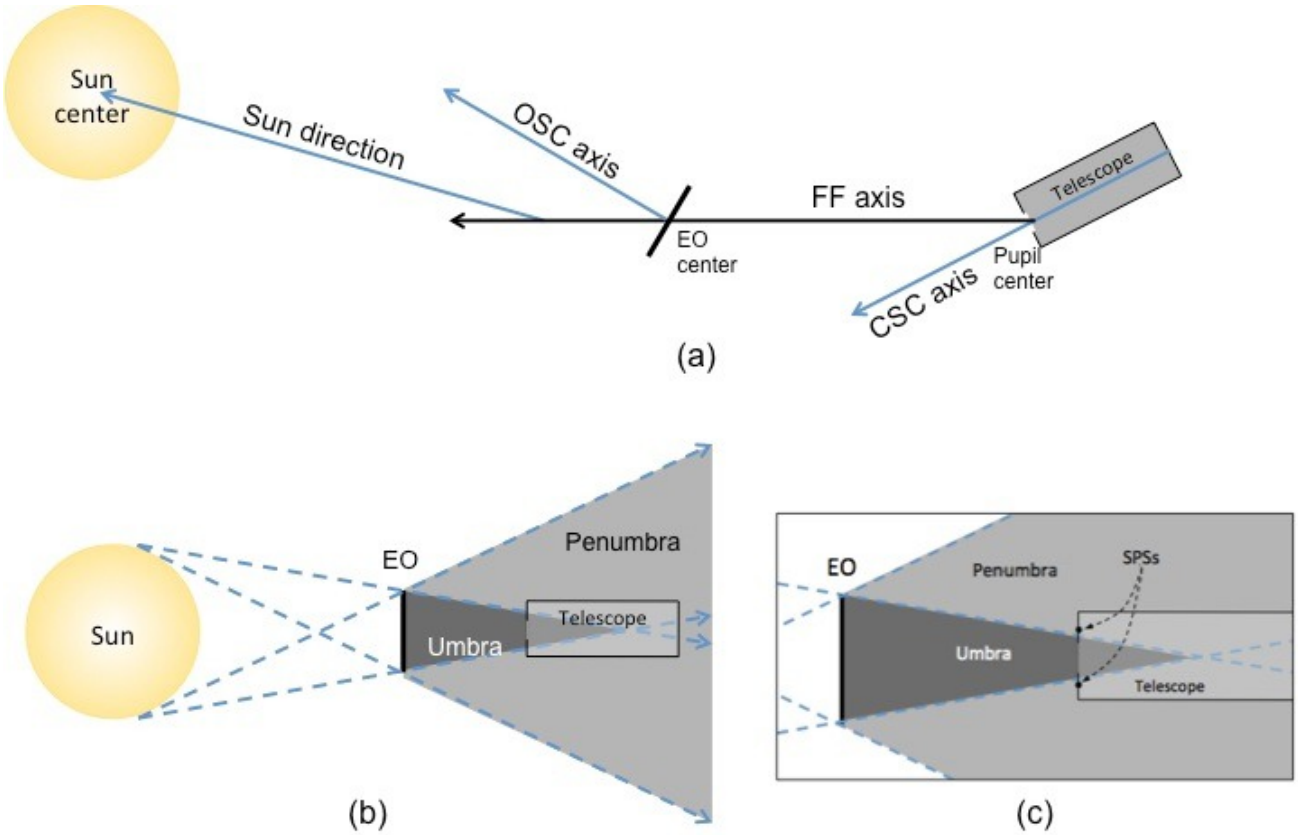

Figure 1. Not-to-scale sketches of the relative position and orientation of the Sun, the EO and the telescope. (a) Definition of the directions and axes for the pointing system(b) Umbra and penumbra geometry. (c) Zoom of figure (b) with emphasis on the SPSs position.

EO edge is by far the smallest ever designed for any flown coronagraph: this will cast down the stray light entering the telescope,[3] with respect to the stray light levels usually experimented by other space born coronagraphs, thus allowing the observation of the corona much closer to the solar disk limb.
The objectives of ASPIICS can be summarized as follows:

- observation of the white-light corona from 1.08 to 3 $R_\odot$ (1 $R_\odot \sim 7 \cdot 10^8$ m) with a minimum spatial resolution of 5.6 arcsec.
- Measurement of the linear polarization of the corona in the wavelength band $540 \div 570$ nm.
- Narrow-band imaging of the inner corona in the He I D3 emission line at 587.6 nm.
- Narrow-band imaging of the corona in the Fe XIV emission line at 530.3 nm.

The performance of the instrument strongly rely on the FF alignment accuracy. The two spacecrafts shall be kept aligned as they constituted a single rigid instrument throughout the whole observing periods.
A dedicated system is designed to take care of the spacecrafts alignment: it accounts for both the absolute pointing of the FF and the relative pointing of the two spacecrafts. As sketched in figure 1 (a), the absolute pointing of the FF corresponds to the alignment of the FF axis with the Sun direction. The Shadow Positioning Sensors (SPSs, described in Sec. 2) account for the absolute pointing by measuring the penumbra around the entrance aperture of the telescope (see figure 1 (b) and (c)): the desired pointing is achieved when the penumbra levels as detected by the SPSs are balanced.

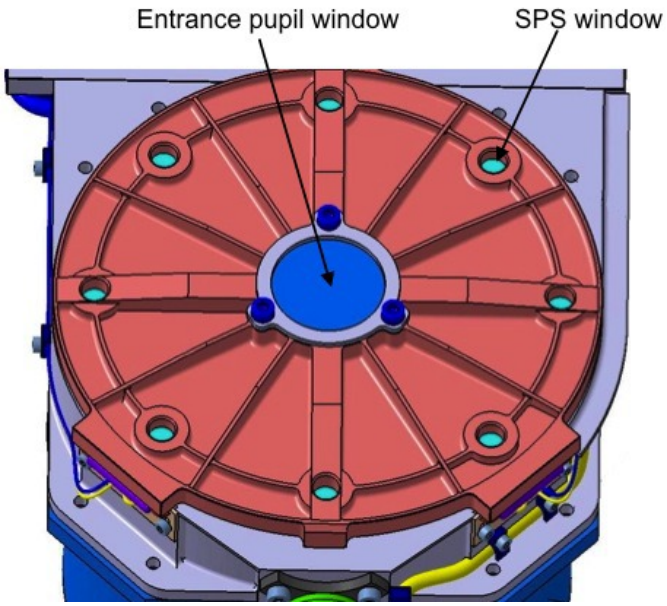

Figure 2. 3D CAD of one of the proposed solutions for the telescope cap (courtesy of Serenum, A.S.). One of the SPS windows is emphasized.

The alignment of the FF corresponds to the alignment of the CSC axis (the optical axis of the telescope) with the FF axis. It can be measured through the coronagraph itself, and its verification can be achieved by quantifying the positioning of the occulter in the field of view of the coronagraph via the Occulter Position Sensor Emitters (OPSE).[2] A set of LED[5] emits light from the back of the EO towards the telescope; their image is directly formed onto the telescope focal plane.
The stray light due to the diffraction from the EO may affect the two metrology systems.

- The detected OPSE signal includes a contribution of stray light with the same physical origin than the stray light affecting coronal images: light that is diffracted by the EO edge and scattered by the telescope optics. It is a contribution that shall be reduced as much as possible, but it is not at risk of jeopardizing the OPSE detection. The position of the leds will be measured anyway, even in presence of a reasonable level of haze introduced by the stray light.
- The signal detected by the SPSs can be highly affected by the stray light. The differential measurements of the SPSs defines the absolute pointing of the system, thus any element that affects the measurement plays a relevant role in the formation fly success. An analysis is being performed on the significance of the diffraction from the EO for the SPSs detection. Section 3 describes such an analysis and its preliminary results.

2. SHADOW POSITION SENSORS

8 Silicon Photomultipliers (SiPM) are disposed on a circumference of radius 55 mm around the telescope entrance pupil. A dedicated investigation has been performed to identify the most suitable number and position of the SPSs to be installed[6] and to optimize their control electronics.[7]
The metrology system shall be able to operate either when the coronagraph is in FF (i.e. thus when the coronal scientific observation is being performed) and when it is not, for radiometric calibration purposes. For this reason, on the front door of the telescope, windows are foreseen in front of the pupil aperture and of the SPSs, as shown in figure 2. The responsivity curve of the SPS is reported in figure 3[6] in A/W, together with the solar irradiance in $\mathrm{Wm^{-2}\ nm^{-1}}$.

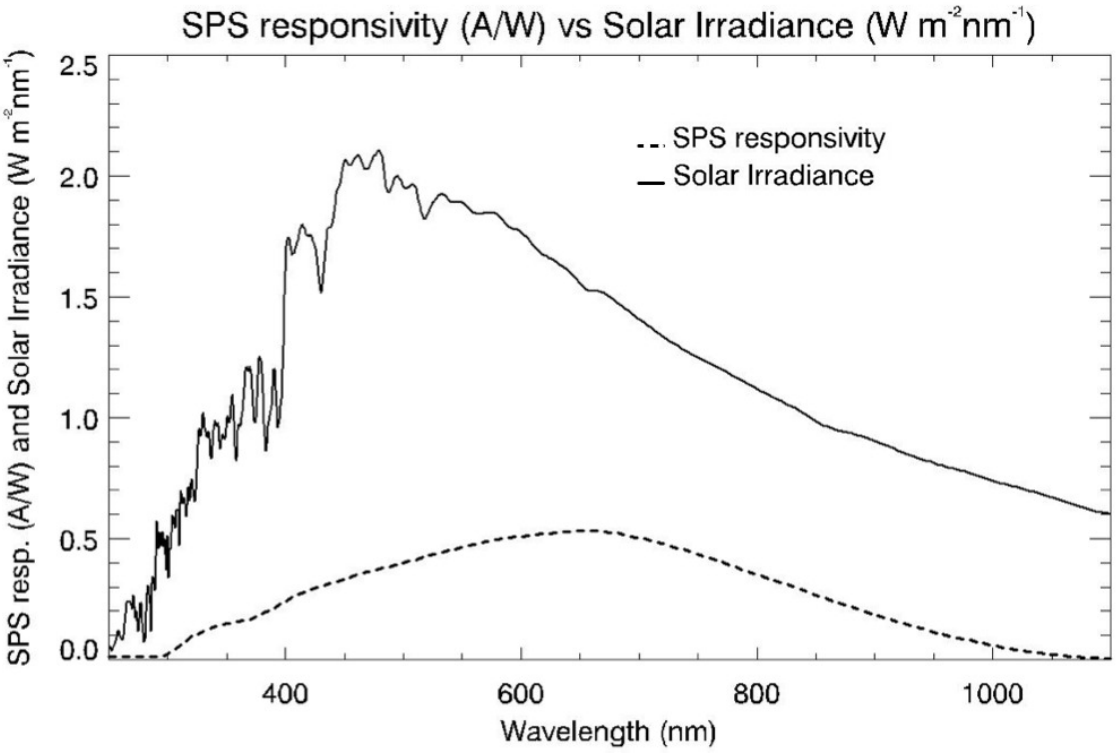

Figure 3. Solid line: solar irradiance. Dashed line: SPS responsivity (courtesy of SensL).

3. DIFFRACTION PATTERN ON THE SPS PLANE

The main component of the light detected by the SPSs is due to the penumbra and has been carefully evaluated on the basis of a geometrical calculation in a dedicated publication.[6] We are here interested in understanding whether the diffraction from the EO is or not significant with respect to the penumbra signal.
Due to the system geometry, the evaluation of the stray light pattern on the SPS plane is a task that requires a huge computational power. While equipping our facilities with the proper hardware and software to be fully dedicated to the investigation (results to be included in a forthcoming publication), we performed a preliminary analysis at a reduced resolution in order to have an indication on the impact of the diffraction contribution to the overall signal detected by the SPSs.
The flight EO is going to have an optimized shape, currently set as a truncated cone,[2,8] but the preliminary analysis was performed with a knife edge disk. The calculation was performed in the following steps:

1) Calculation of the diffraction produced by the knife edge EO on the SPS plane for a single point source in the center of the solar disk (impinging plane wave parallel to the SPS plane).

2) Convolution of the diffraction of step (1) with a solar disk kernel with the dimension of the solar disk on the SPS plane, in order to calculate the diffraction with the whole solar disk as a source, normalized to the mean solar disk brightness. The calculation is performed at a fixed wavelength. The kernel includes a wavelength-dependent limb darkening model.[9]

3) Steps (1) and (2) are repeated for a set of wavelengths in order to sample the responsivity curve of the SPSs (figure 3).

4) The patterns obtained at step (3) are integrated over the wavelength with weight factors given by the appropriate value according to the solar irradiance (figure 3) and to the SPS responsivity.

The final result is a preliminary evaluation of the whole signal detected by the SPS, including the diffraction effects that cannot be taken into account by pure geometrical analyses.[6]
Sections 3.1 and 3.2 are dedicated to a more thorough description of the listed steps.

3.1 Diffraction with the whole solar disk as a source

The diffraction calculation of step (1) is performed by numerically evaluating the well known Fresnel-Kirchhoff diffraction integral[10] on a plane positioned 144.348 m behind a 1.42 m opaque disk:

$$\mathrm{D_p(r,\lambda) = |U(r,\lambda)|^2 \simeq \left| \frac{-2\mathrm{Ai}}{\lambda} \frac{e^{ikz}}{z} \iint_S e^{ik\frac{\xi^2+\eta^2}{2z}} d\xi d\eta \right|^2} \quad (1)$$

where $\mathrm{U(r,\lambda)}$ is the value of the electro-magnetic field at a radial distance r on the image plane (the diffraction pattern has circular symmetry), S is the integration surface on the external occulter plane, λ is the wavelength, z=144.348 m is the distance between the EO and the image plane, η and ξ are orthonormal coordinates on the EO plane. In order to retrieve equation (1), a source at infinity has been considered, the close field approximation has been adopted and the origin of the frame of reference has been set at the intersection of the source-image point line with the EO plane. The radial coordinate r has its origin on the optical axis (in the center of the coronagraph entrance aperture).

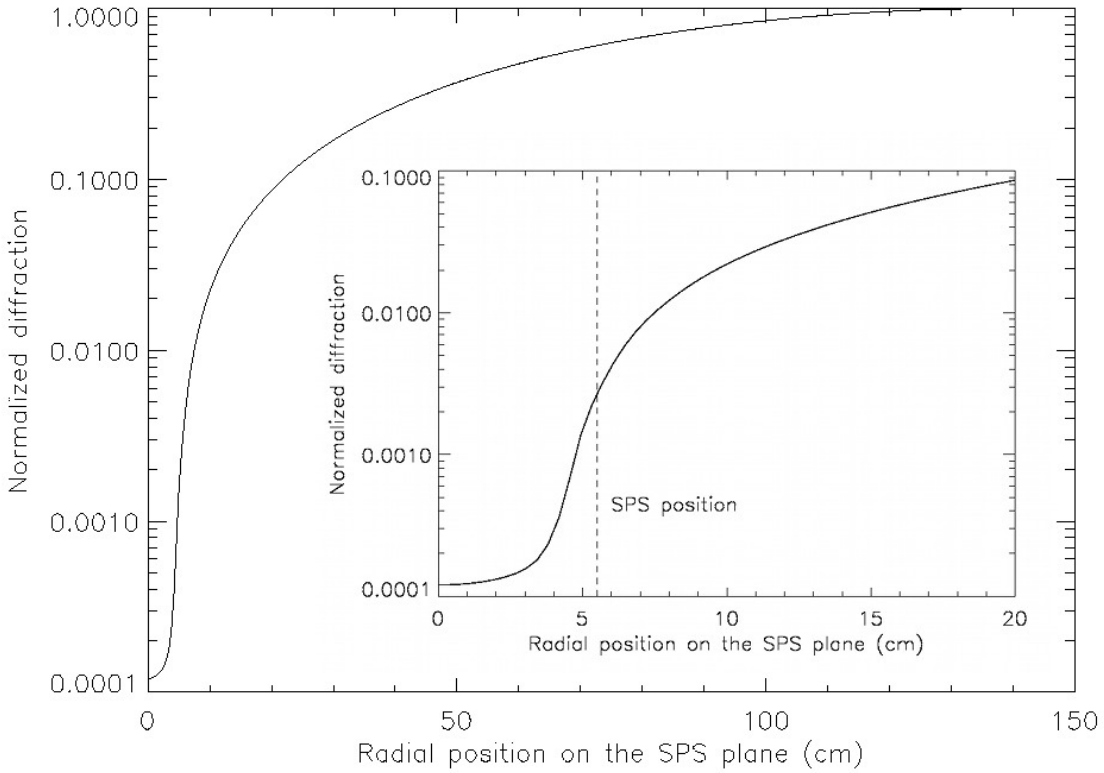

Figure 4. Diffraction profile on the SPS plane as generated by the whole solar disk behind the EO, for a fixed wavelength of 550 nm. In the smaller plot, a zoom of the region closer to the optical axis is shown.

The resulting pattern is convolved (step (2)) with a solar disk kernel with the dimension of the solar disk on the SPS plane (diameter $\sim$ 1.345 m):

$$\mathrm{D(r,\lambda) = B \int_0^{2\pi} d\hat{\phi} \int_0^{R_{Disk}} D_p(r-\rho, \hat{\phi}-\phi, \lambda) Disk(\rho,\phi,\lambda) \rho d\rho} \quad (2)$$

where $R_{Disk} \simeq 0.672$ m is the radius of the projection of the solar disk on the SPS plane; $Disk(\rho, \phi, \lambda) = Disk(\rho, \lambda)$ is the circularly symmetric function that defines the irradiance of the solar disk at a given wavelength λ; it is 0 for ρ greater than the projection of the solar radius on the SPS plane. B is a normalization constant.
The following limb darkening model is included in the expression of $Disk(\rho, \lambda)$:[9]

$$L(\theta, \lambda) = 1 - u_2(\lambda) - v_2(\lambda) + u_2(\lambda) \cos\theta + v_2(\lambda) \cos^2\theta \tag{3}$$

where θ is the angle between the solar radius vector and the line of sight, while u_2 and v_2 are tabulated wavelength-dependent parameters.[9] The resulting profile, normalized to the solar disk brightness, for a wavelength λ=550 nm, is shown in figure 4. The SPS position is emphasized by a vertical dashed line. As foreseen (see Sec. 2 and figure 1), the SPSs lay in the penumbra.
In order to show the reliability of our algorithm, we compared our result with one of the most recent on the same topic present in literature,[11] in the same case of umbra and penumbra dimensions, at a wavelength of 550 nm. We adapted the geometry of our simulation to the same case treated in literature, i.e., an occulter of 1.5 m diameter and an image plane at a distance of 150.4 m. Figure 5 shows the comparison.

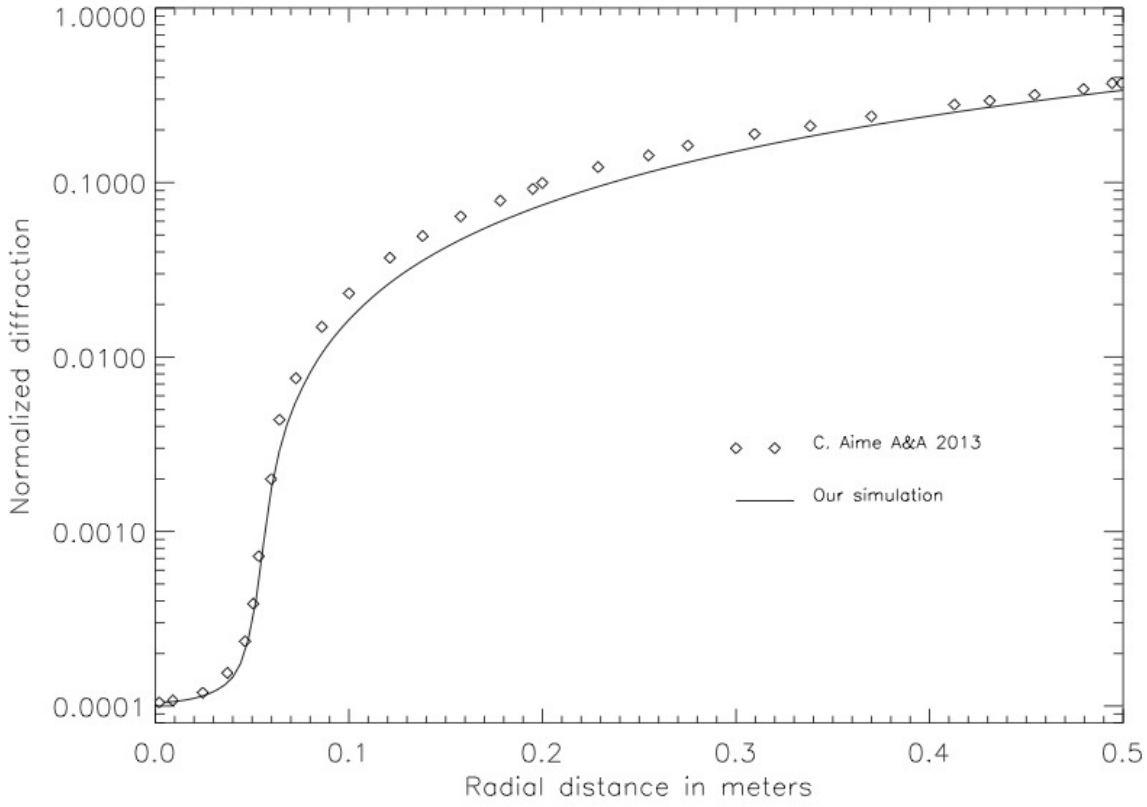

Figure 5. Comparison of our algorithm result with the literature,[11] for an occulter of 1.5 m diameter at 150.4 m from the image plane.

3.2 Signal detected by a SPS

Since SPSs are designed to lay in the penumbra, the main contribution to the signal that they should detect can be calculated with an accurate geometrical analysis that considers the portion of the Sun that emerges from the EO. A dedicated publication reports on the geometrical analysis[6] and its result is included here as a comparison. Profiles at a fixed wavelength (like the one shown in figure 4) are calculated for a set of wavelengths sampling the sensitivity range of the SPSs (figure 3).

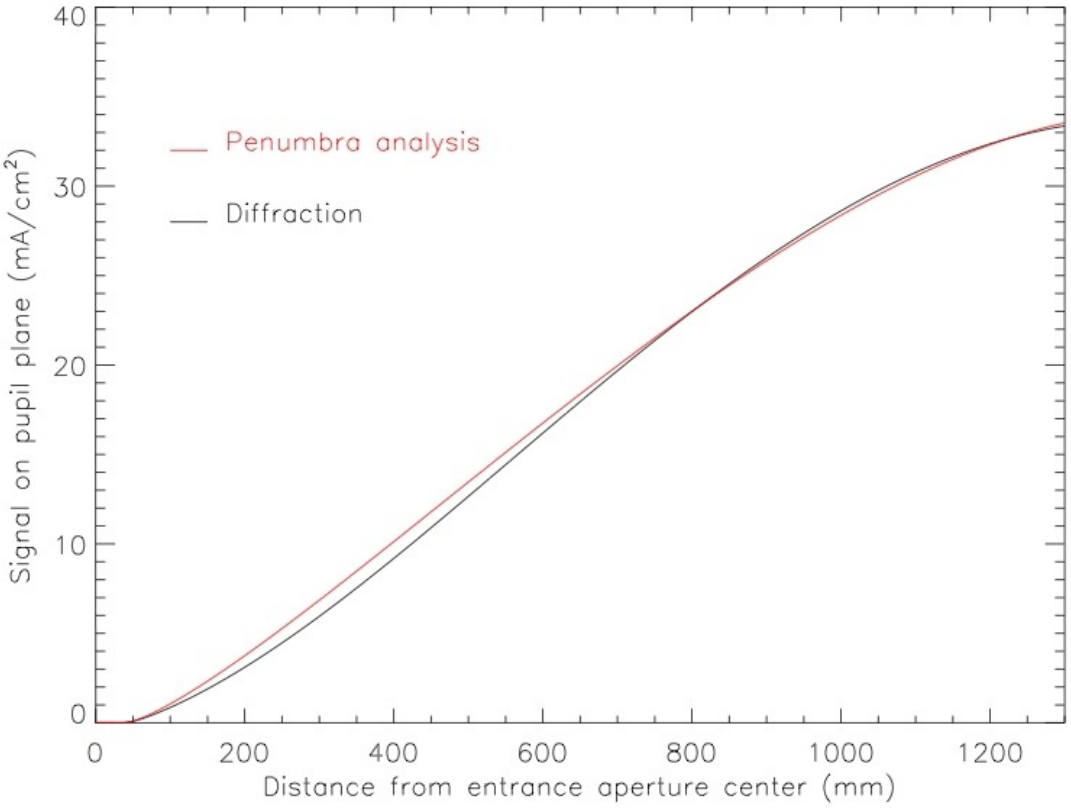

Figure 6. Signal on the SPS plane. Comparison between the geometrical penumbra calculation (red) and the diffraction calculation (black).

Each profile is weighted for the solar irradiance and the SPS responsivity and summed to the others, in order to numerically evaluate the following integral:

$$\mathrm{I(r)} = \int_{\lambda} \mathrm{D(r,\lambda)\ I_{\odot}(\lambda)\ R_{SPS}(\lambda)\ d\lambda} \tag{4}$$

where r is the radial position on the SPS plane, I(r) is the signal detected by a SPS that is at distance r from the optical axis, $\mathrm{D(r,\lambda)}$ is the diffraction profile for a certain wavelength λ, $\mathrm{I_{\odot}}$ is the solar irradiance and $\mathrm{R_{SPS}}$ is the SPS responsivity.

Figures 6 and 7 show the resulting profile. The result of the geometrical calculation is included as well. The two profiles show a good agreement over the SPS plane, except for the umbra range, where the geometrical calculation result cannot be different from 0.
In principle, the diffraction calculation should include both the penumbra and the diffraction contribution, thus in the penumbra range the black curve should be slightly greater than the red one (figure 7): we ascribe the discrepancy to the lack of resolution of the diffraction calculation (a similar discrepancy is also shown in figure 5). It will be probably fixed in the more accurate calculations that are going to be performed with appropriate hardware and software tools.

4. SIGNIFICANCE OF THE DIFFRACTION FOR THE FF ALIGNMENT

The diffraction curve (figure 7) has the same order of magnitude of the geometrically calculated penumbra in the position range where the SPSs will operate (55 mm from the entrance aperture center).[6] The slope of the two

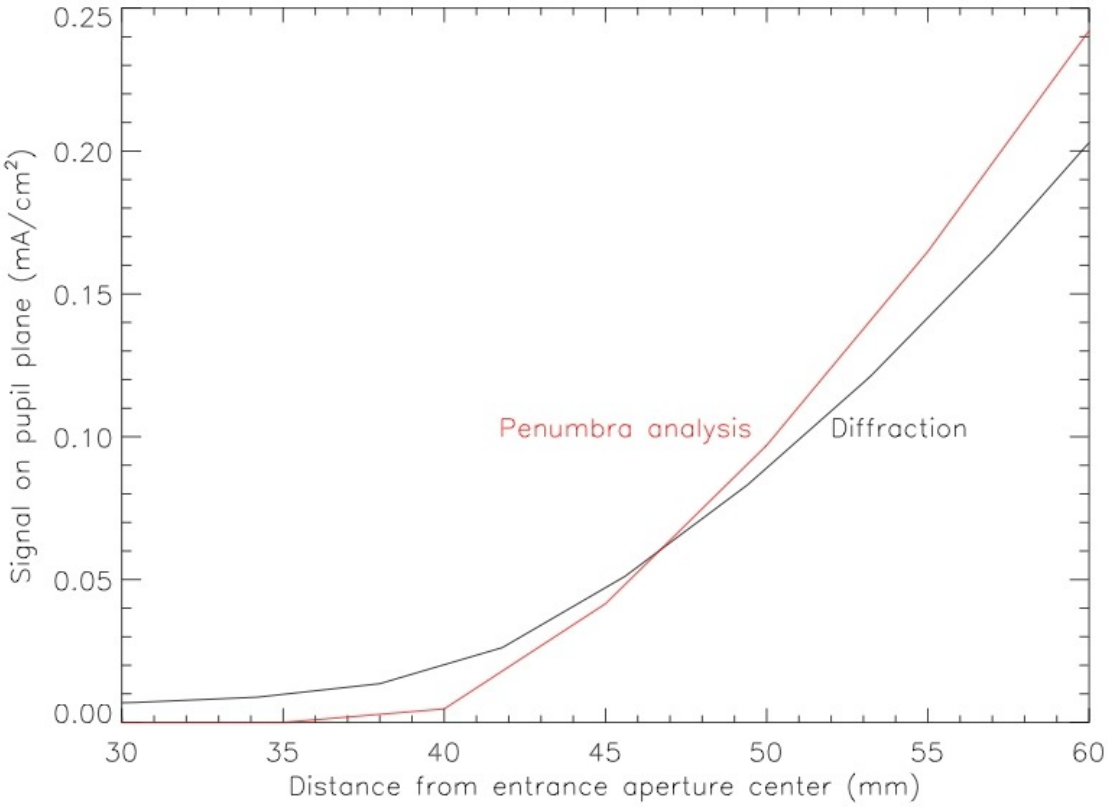

Figure 7. Signal on the SPS plane. This plot show a particular of figure 6 in the range of interest for the SPS position (55 mm from the entrance aperture center).

curves is similar as well, and this allows us to validate the discussion of Bemporad et al.[6] on the FF alignment algorithm. In order to understand which is the impact of the diffraction from EO on the FF mispositioning along the FF axis, we performed a preliminary investigation at low resolution (to limit the computational time within reasonable constraints) by repeating the simulation described in Sec. 3.2 at different inter-satellite distances (ISDs). For each plot we extrapolated the signal at the SPS position and we evaluated the percent variation with respect to the value in the nominal ISD case:

$$\Delta I(\Delta_{ISD}) = \frac{I(r_{SPS}) - I_{\Delta_{ISD}}(r_{SPS})}{I(r_{SPS})} \cdot 100 \tag{5}$$

where $I(r_{SPS})$ is the value of the diffraction curve of figures 6 and 7 in correspondence of the SPS position (r_{SPS}=55 mm), $I_{\Delta_{ISD}}$ is the diffraction curve evaluated at ISD=144348 mm $+\Delta_{ISD}$. Figure 8 shows the resulting percent variation as a function of Δ_{ISD}. The positive deviations from the nominal ISD have no significative impact on the signal detected by the SPSs. The negative deviations are detected by the SPSs as a positive and roughly constant bias.

5. CONCLUSIONS

A preliminary analysis has been performed on the significance of the diffraction from the external occulter on the formation fly metrology for the PROBA-3/ASPIICS coronagraph. At a first evaluation, it seems that the diffraction has not a significative impact on the SPSs signal detection for mis-alignments perpendicular to the coronagraph optical axis. Positive deviations from the nominal inter-satellite distance do not significantly affect the SPSs signal. Negative deviations from the nominal inter-satellite distance are detected as a roughly constant

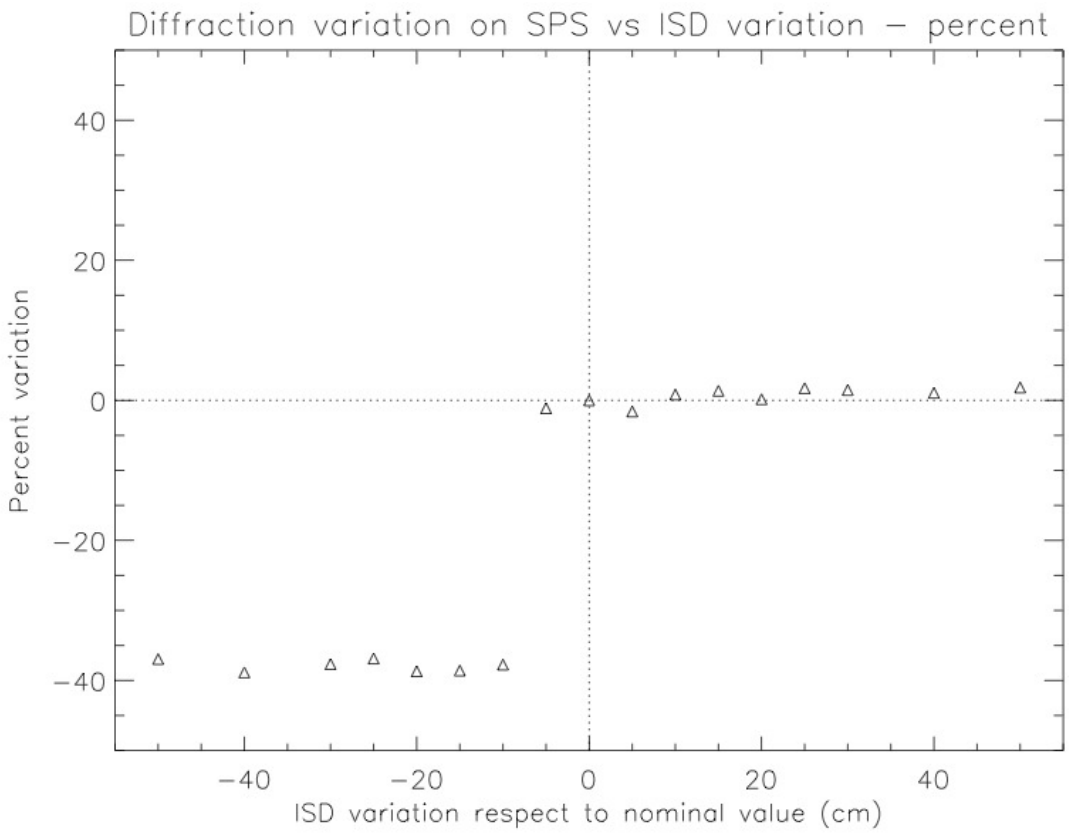

Figure 8. Percent variation (equation (5)) of the diffraction value at the SPS position as a function of the displacement from the nominal ISD.

positive bias.
The present analysis shall not be considered conclusive and shall be confirmed by forthcoming more accurate ones, that are being performed with proper hardware and software tools.
Moreover, the final analysis will possibly have to take into account the optimization of the external occulter, that is not considered in the preliminary calculation. In fact, the external occulter will be characterized by an optimized shape (currently set as a truncated cone[8]), designed in order to achieve a further reduction of the stray light level on the focal plane.

ACKNOWLEDGMENTS

The ASPIICS project will be developed under the auspices of the ESA's General Support Technology Programme (GSTP) and the ESA's Prodex Programme thanks to the sponsorships of seven member states: Belgium, Poland, Romania, Italy, Ireland, Greece, and the Czech Republic.

REFERENCES

[1] Lyot, B., "Étude de la couronne solaire en dehors des éclipses. Avec 16 figures dans le texte.," *Zeitschrift fur Astrophysics* **5**, 73 (1932).
[2] Renotte, E. et al., "Design status of ASPIICS, an externally occulted coronagraph for PROBA-3," *Proc. SPIE* **9604**, in press (2015).
[3] Vives, S. et al., "Formation flyers applied to solar coronal observations: the ASPICS mission," *Proc. SPIE* **5901**, 590116.1–11 (2005).

[4] Evans, J. W., "Photometer for measurement of sky brightness near the sun," *J. Opt. Soc. Am.* **38**, 1083 (1948).
[5] Loreggia, D. et al., "OPSE metrology system onboard of the PROBA3 mission of ESA," *Proc. SPIE* **9604**, in press (2015).
[6] Bemporad, A. et al., "The shadow positioning sensors (SPS) for formation flying metrology on-board the ESA-PROBA3 mission," *Proc. SPIE* **9604**, in press (2015).
[7] Focardi, M. et al., "Formation flying metrology for the ESA-PROBA3 Mission: the shadow position sensors (SPS) silicon photomultipliers (SiPMs) readout electronics," *Proc. SPIE* **9604**, in press (2015).
[8] Landini, F. et al., "External occulter laboratory demonstrator for the forthcoming formation flying coronagraphs," *App. Opt.* **50**, 6632–6644 (2011).
[9] Cox, A. N., [*Allen's Astrophysical Quantities*], AIP press, Springer-Verlag, New York (2000).
[10] Born, M. and Wolf, E., [*Principles of Optics*], Cambridge University Press, Cambridge (2001).
[11] Aime, C., "Theoretical performance of solar coronagraphs using sharp-edged or apodized circular external occulters," *A&A* **558**, A138.1–10 (2013).